Giovanni Casotti, Kimberly K. Lindberg and Eldon J. Braun
Am J Physiol Regulatory Integrative Comp Physiol 279:1722-1730, 2000.

You might find this additional information useful...

This article cites 26 articles, 9 of which you can access free at:
http://ajpregu.physiology.org/cgi/content/full/279/5/R1722#BIBL

This article has been cited by 1 other HighWire hosted article:
Crucial roles of Brn1 in distal tubule formation and function in mouse kidney
S. Nakai, Y. Sugitani, H. Sato, S. Ito, Y. Miura, M. Ogawa, M. Nishi, K.-i. Jishage, O. Minowa and T. Noda
Development, October 1, 2003; 130 (19): 4751-4759.
[Abstract] [Full Text] [PDF]

Medline items on this article's topics can be found at http://highwire.stanford.edu/lists/artbytopic.dtl on the following topics:
Physiology .. Kidneys
Physiology .. Renal Medulla
Physiology .. Nephrons
Physiology .. Loop of Henle
Medicine .. Microscopy

Updated information and services including high-resolution figures, can be found at:
http://ajpregu.physiology.org/cgi/content/full/279/5/R1722

Additional material and information about ***American Journal of Physiology - Regulatory, Integrative and Comparative Physiology*** can be found at:
http://www.the-aps.org/publications/ajpregu

This information is current as of July 31, 2007 .

The American Journal of Physiology - Regulatory, Integrative and Comparative Physiology publishes original investigations that illuminate normal or abnormal regulation and integration of physiological mechanisms at all levels of biological organization, ranging from molecules to humans, including clinical investigations. It is published 12 times a year (monthly) by the American Physiological Society, 9650 Rockville Pike, Bethesda MD 20814-3991. Copyright © 2005 by the American Physiological Society. ISSN: 0363-6119, ESSN: 1522-1490. Visit our website at http://www.the-aps.org/.

Downloaded from ajpregu.physiology.org on July 31, 2007

Am J Physiol Regulatory Integrative Comp Physiol
279: R1722–R1730, 2000.

Functional morphology of the avian medullary cone

GIOVANNI CASOTTI,[1] KIMBERLY K. LINDBERG,[2] AND ELDON J. BRAUN[2]
[1]*Department of Biology, West Chester University, West Chester, Pennsylvania 19383; and* [2]*Department of Physiology, University of Arizona, Tucson, Arizona 85724*

Received 12 July 1999; accepted in final form 9 June 2000

Casotti, Giovanni, Kimberly K. Lindberg, and Eldon J. Braun. Functional morphology of the avian medullary cone. *Am J Physiol Regulatory Integrative Comp Physiol* 279: R1722–R1730, 2000.—The organization of the renal medulla of the Gambel's quail, *Callipepla gambelii*, kidney was examined to determine the number of loops of Henle and collecting ducts and the surface area occupied by the different nephron segments as a function of distance down the medullary cones. Eleven medullary cones were dissected from the kidneys of four birds, and the tissue was processed and sectioned for light microscopy. In addition, individual nephrons were isolated on which total loop thin descending segment and thick prebend segment lengths were measured. The results show no correlation between the absolute number of loops of Henle and the length of the medullary cones. The number of thick and thin limbs of Henle and collecting ducts decrease exponentially with distance toward the apex of the cones and the rate of decrease is similar for cones of different lengths. Initially there is a rapid decrease in the number of thin limbs of Henle, indicating that most nephrons do not penetrate the cones a great distance. Thick descending limbs of Henle (prebend segment) ranged in length from 50 to 770 μm, and there was little correlation with the total length of the loop of Henle. However, the length of the thin limb of Henle correlated well with total loop length. The cell surface areas of the limbs of the loop of Henle and the collectng ducts decreased toward the apex of the cones.

bird; kidney; nephron; loop of Henle; collecting duct; urine concentration

OUR CURRENT UNDERSTANDING of urine concentration through countercurrent multiplication is based almost solely on data for the kidneys of mammals. Some of what has been learned about the renal countercurrent mechanism of the mammalian kidney has been derived from mathematical models and computer simulations (23). Because there are some differences in the morphology of the looped nephrons of the avian kidney and those of mammals, it may not be appropriate to apply existing modeling studies of the mammalian kidney to the avian kidney. These differences, plus the lack of quantitative morphological data for the medullary region of the avian kidney, prompted the current investigation. The aim of the present study was to determine the gradation in loop of Henle length, the coalescence of collecting ducts, and the surface area occupied by the different tubule elements at successive levels from the base to the apex of avian medullary cones.

Aside from mammals, birds are the only group of vertebrates that conserve body water by producing urine osmotically more concentrated than the plasma from which it is derived. However, this ability by birds to concentrate urine is limited compared with that of mammals. Typically, water-deprived birds produce urine that is 2.0–2.5 times more concentrated than plasma, whereas some mammals are capable of producing urine that is 20–25 times more concentrated than plasma (11, 17, 18). To explain these differences, the variation in the organization of the kidneys of birds and mammals should be examined.

Gross kidney structure in mammals ranges from the simple unipapillate of small mammals to the compound multirenculate kidneys found in large marine mammals (10). Despite this range in structure the basic organization of the mammal kidney is maintained and consists of a central medulla that is surrounded by an outer cortex. In contrast, the avian kidney consists of a series of lobules each containing a cortex and a medulla that is shaped like a cone (the medullary cones; Refs. 3, 5, 20). The medullary cones (renal medulla) are not divided into inner and outer regions, as is the case for the kidneys of some mammals.

Although differences in the gross morphology of the renal medulla between mammals and birds are apparent, both medullae contain nephrons with a loop of Henle. Although all nephrons within the mammal kidney contain a loop, in birds only a small percentage of nephrons (10–30%) contain a loop of Henle (i.e., looped nephrons) (4). The remaining large population of nephrons in the avian kidney does not have a loop of Henle. The cortex of the avian kidney is made up of the proximal tubules of the looped nephrons and the large number of nephrons without a loop of Henle (loopless nephrons). In mammal kidneys, the numbers of collecting ducts decrease with distance down the renal medulla. The same is true in the medullary cones of the avian kidney. Moreover, in the avian kidney, the collecting ducts from the loopless nephrons merge in the medullary cones with those of the looped nephrons (3).

Address for reprint requests and other correspondence: G. Casotti, Dept. of Biology, West Chester Univ., West Chester, PA 19383 (E-mail: giovanni@bio.wcupa.edu).

The costs of publication of this article were defrayed in part by the payment of page charges. The article must therefore be hereby marked "*advertisement*" in accordance with 18 U.S.C. Section 1734 solely to indicate this fact.

 0363-6119/00 $5.00 Copyright © 2000 the American Physiological Society

Downloaded from ajpregu.physiology.org on July 31, 2007

Although all the nephrons in mammal kidneys have a loop of Henle, the structure of the loop depends to a degree on the point at which the hairpin loop is formed. The very short nephrons have short, thin descending segments and thick epithelial cells may form the hairpin loop. For the longer nephrons, thin epithelial cells form the hairpin loop (1, 2). In the avian kidney, the hairpin loop of all the looped nephrons consists of thick epithelial cells, i.e., the epithelium of the avian loop of Henle always thickens prior to the hairpin turn (21).

Concentration of the urine by the mammalian kidney is achieved by the parallel arrangement of nephron elements in the renal medulla that function as a countercurrent multiplier. In this system, the tubule fluid is diluted by the active reabsorption of solute (sodium chloride) from the ascending thick limb of Henle without the simultaneous removal of water from the tubule. Deposition of solutes (sodium chloride and urea) in the medullary interstitium creates an environment that is hyperosmotic to the plasma. As the tubule fluid descends in the collecting ducts, antidiuretic hormone facilitates the movement of water to the hyperosmotic interstitium. The function of the thin ascending limb of Henle in this countercurrent multiplier system is unclear (9, 23). The avian kidney has a similar parallel arrangement of the loops of Henle and collecting ducts in the medullary cones, making it likely that it also concentrates urine by a countercurrent multiplier system. However, the intramedullary osmotic gradient of the medullary cones consists of a single solute, sodium chloride (12, 25). The avian countercurrent multiplier system is further complicated and possibly compromised because the collecting ducts in the medullary cones receive fluid from nephrons in the renal cortex that do not have loops of Henle (3). The fluid from these nephrons may be hypotonic or at best isotonic to plasma.

Several mathematical models have been proposed in an attempt to explain the way the mammalian countercurrent multiplier system functions (22, 26–28). In contrast, only one modeling study has examined the countercurrent multiplier system within the avian kidney (16). A second, less quantitative model was proposed for the avian countercurrent multiplier system (19). In this study, the authors used available anatomic and physiological data to propose a model based on a cascade in the length of the loops of Henle with distance down the medullary cones and the observation that sodium chloride is the only solute in the medullary osmotic gradient. However, it did not account for variation in the length of the thin descending segment or the presence of a thick prebend segment to the loop of Henle.

Like mammals, the loop of Henle in birds varies in length among nephrons; however, the pattern of loop formation with depth down the medullary cone has not been examined. Two studies on mammals (one on the rat, the other on the rabbit) have examined the pattern of nephron looping as a function of medullary depth (14, 24). The pattern of loop formation in the medulla may be important to understanding how renal countercurrent multiplier systems operate. Differences in the number of nephrons as a function of medullary depth have been examined in mammals by Knepper et al. (14). Changes in number of nephrons as a function of medulla depth could be responsible for considerable differences in the quantities of solute and water transported and thus urine concentrating ability (14). The study on the avian kidney reported in the present paper is analogous to that of Knepper et al. (14).

The present study was undertaken in anticipation that the results would lead to a better understanding of the urine concentrating mechanism of the avian kidney. Furthermore, the data should be useful in constructing mathematical models and computer simulations of the system.

MATERIALS AND METHODS

Gambel's quail were collected under state license using a funnel box trap in the vicinity of Tucson, Arizona. This species was chosen because of the large database that exists on the nephron population of its kidneys (3, 6, 7, 21, 29).

Four birds were euthanized with intraperitoneal injections of pentobarbital sodium (0.5 ml of 50 mg/ml stock). The abdomen of each bird was opened by a single medial ventral incision, and the viscera was removed to expose the kidneys. The dorsal aorta was cannulated just cranial to the kidneys, and blood was flushed from the kidneys with phosphate buffer (pH 7.4). To ensure optimum fixation of the renal medulla, the kidneys were perfused-fixed with half-strength Karnovsky's fixative at an osmolality of 750 mosmol/kgH_2O. Both kidneys were removed from the synsacrum and stored in the perfusion fixative overnight at room temperature.

For each animal, all of the medullary cones were dissected from both kidneys. They were placed in a petri dish, and cones were selected at random for analysis. The cones were embedded in paraffin wax and processed routinely for light microscopy. Serial transverse sections were cut through the length of the cones at a thickness of 5 μm. The sections were mounted on glass slides and stained with hematoxylin and eosin. A total of 11 cones that ranged in length from 950 to 3,350 μm from the eight kidneys of four birds were examined (~3 from each bird). The mean length of all cones was 1,654 ± 738 μm. On average, a single Gambel's quail kidney contains 48 cones, thus we sampled ~3% of the cones in the eight kidneys.

The histological sections were sampled at 50-μm intervals (every tenth section) for the length of the cones. Sampling began at the base of the cones, which corresponded to the corticomedullary boundary and continued to the apex (tip) of the cones (Fig. 1). A Sony charged coupled device camera mounted on an Olympus BH-2 microscope was used to project the sections onto a video monitor. The images were captured using a Targa True Vision frame grabber and analyzed using an image analysis program (Sigma Scan; Jandel, San Rafael, CA). At each level, the numbers of tubule elements were counted (thin and thick limbs of Henle and collecting ducts). For each tubule, the inside and outside diameters were measured (Fig. 1). These data were used to calculate the cross-sectional cell surface area of each tubule using the formula for calculating the surface area of an annulus [$A = \Pi (r_1 + r_2)(r_1 - r_2)$, where $r_1 \geq r_2$]. These data are presented in Table 1.

In addition to the histology, direct quantitative data on the length of the thin limb of Henle and the prebend segment were generated by dissecting 59 looped nephrons from the medullary cones of an additional five Gambel's quail. Birds

Downloaded from ajpregu.physiology.org on July 31, 2007

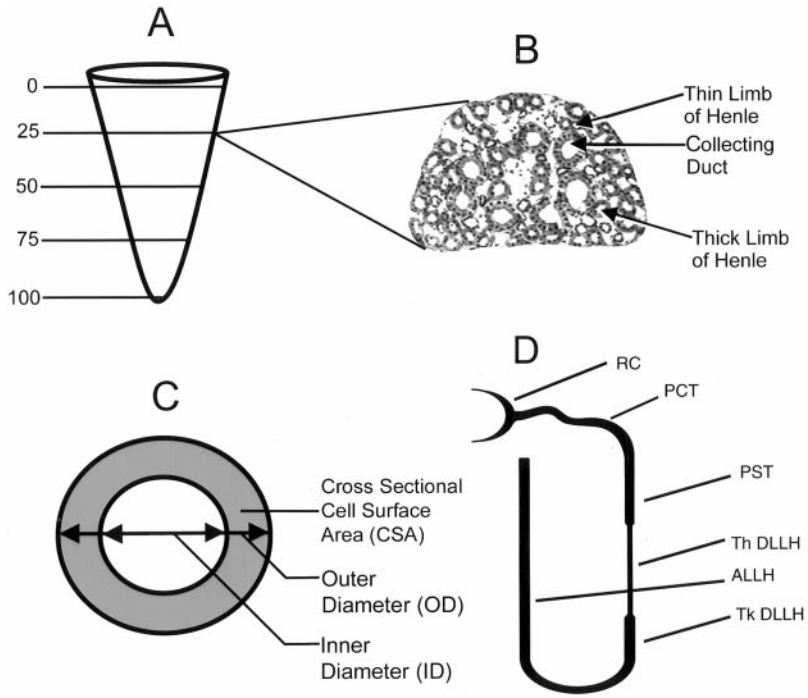

Fig. 1. *A*: schematic showing the division of an avian medullary cone into fractional depths. *B*: a single cross-section of a cone showing the different tubule types. *C*: parameters measured for each tubule type. Measurements of the inner and outer diameters were made using imaging software (Jandel Sigma Scan Pro), and the data were used to calculate the cross-sectional surface area of each tubule type. The tubules were treated as an annulus and the formula [$A = \Pi (r_1 + r_2) (r_1 - r_2)$, where $r_1 \geq r_2$] was used to calculate the cross-sectional surface area. *D*: schematic of an avian looped nephron. Note that the epithelium thickens before the hairpin loop is formed. RC, renal corpuscle; PCT, proximal convoluted tubule; PST, proximal straight tubule; Th DLLH, thin descending limb of the loop of Henle; ALLH, ascending limb of the loop of Henle; Tk DLLH, thick descending limb of the loop of Henle.

were prepared as described earlier; however, instead of perfusion fixation, fresh kidneys were dissected from the synsacrum and immersed in a solution of alcoholic ferric chloride (95 ml ethyl alcohol, 5 ml concentrated HCl, 30 g ferric chloride) overnight at 4°C. This was followed by digestion for 2 h in 20% HCl at 37°C, after which the tissue was placed in cold (4°C) acid ferric chloride (200 mg ferric chloride, 0.2 ml acetic acid, and 100 ml distilled water). The kidneys were rehydrated in water for 4–12 h, and individual nephrons were dissected free using finely drawn glass needles. The nephrons were transferred to a drop of 50% glycerol on a microscope slide, and the outline of the nephrons was drawn with the use of a camera Lucida attached to a microscope. The total length of the loop of Henle and the lengths of the thin limb of Henle and prebend segment were measured using the imaging software previously mentioned.

RESULTS

The renal medulla of birds is composed of a number of small units, the medullary cones. As demonstrated in this study, the cones vary widely in diameter at the base, total length, number of loops of Henle, and in the number of collecting ducts. Because of the large variation in these parameters, it would confer little biological value to present the data as means across the cones. However, and as is typical for the desert quail, the internal organization of the cones is very consistent within a given species. This architecture of the cones can be seen in Fig. 2, which contains scanning electron micrographs of methyl methacrylate casts of the loops of Henle and collecting ducts. Figure 2*A* clearly shows the pattern of coalescence that occurs in the collecting duct system. This coalescence appears not to be random but occurs at specific nodal points, and it appears that this pattern holds for all the collecting ducts in a cone. Inspection of the data in Table 1 on the number of collecting ducts with medullary cone depth also reinforces this pattern of convergence. For example, the number of collecting ducts in cone three decreases in the following pattern: 19, 12, 8, 4, 2. This dichotomous pattern of coalescence has been observed previously for the desert quail and the domestic chicken (3).

Numerical data describing the composition of the eleven medullary cones are presented in Table 1. The data are expressed as a function of fractional depth of the cones with the absolute length of the cones taken as 100% and the corticomedullary boundary as zero. As pointed out previously, there is a great deal of variation in the length of the cones within a kidney of species. This is apparent as we present data on cones that ranged in length from 950 to 3,350 μm. There was also variability in the number of nephrons among the cones. Shorter cones did not always have a smaller number of nephrons and vice versa. This is evident when the relationship between number of loops for each cone and cone length is examined ($r = 0.27$, Fig. 3).

In all cones the number of thick limbs of Henle was the greatest at the base and showed a rapid, exponential decrease toward the apex of the medullary cones (Table 1). This point is shown graphically for one cone (cone 11) in Fig. 4*A*. In all cases, the decrease in the number of thin limbs of Henle toward the apices of the cones was more rapid than the decrease in number for the thick limbs of Henle (Figs. 4*A* and 7; Table 1). Moreover, there was little correlation between the number of thin limbs and the length of the medullary cones ($r = -0.25$, $P < 0.05$).

The number of collecting ducts was greatest at the base of the cones and showed a rapid decrease toward

Downloaded from ajpregu.physiology.org on July 31, 2007

Table 1. *Morphological parameters of the tubule elements within the medullary cones of the desert quail*

Relative Depth (%)	Thick Limb of Henle					Thin Limb of Henle					Collecting Ducts				
	n	ID	OD	CSA	%CSA	*n*	ID	OD	CSA	%CSA	*n*	ID	OD	CSA	%CSA
Cone 1, 950 μm															
0	192	1,753	4,013	10.235	100	99	676	1,295	0.958	100	36	1,887	3,617	7.478	100
25	111	981	2,376	3.678	35.9	69	471	836	0.375	39.1	27	553	1,162	0.820	11.0
50	84	690	1,710	1.923	18.8	37	215	420	0.102	10.7	20	443	913	0.501	6.7
75	34	360	762	0.354	3.5	15	112	193	0.019	2.0	7	218	507	0.165	2.2
100	23	231	530	0.179	1.7	11	62	126	0.009	1.0	4	141	348	0.080	1.1
Cone 2, 1,050 μm															
0	203	1,949	4,433	12.451	100	95	609	1,216	0.870	100	38	817	1,704	1.756	100
25	88	991	2,055	2.545	20.4	49	326	627	0.225	25.9	23	587	1,262	0.980	55.8
50	73	731	1,599	1.588	12.8	39	247	475	0.129	14.9	18	512	1,128	0.793	45.2
75	34	369	829	0.433	3.5	16	100	195	0.022	2.5	9	307	617	0.225	12.8
100	11	174	346	0.070	0.6	1	10	13	0	0.0	4	103	246	0.039	2.2
Cone 3, 1,100 μm															
0	65	655	1,650	1.801	100	11	72	180	0.021	100	19	441	846	0.409	100
25	48	409	1,021	0.687	38.2	9	52	106	0.007	31.3	12	274	511	0.146	35.7
50	29	316	745	0.357	19.8	13	42	142	0.014	67.6	8	241	395	0.077	18.8
75	21	223	604	0.247	13.7	4	9	34	0.001	3.9	4	193	272	0.029	7.0
100	8	108	341	0.082	4.6	0	0	0	0	0.0	2	222	318	0.041	9.9
Cone 4, 1,150 μm															
0	29	331	802	0.419	100	4	48	84	0.004	100	7	160	312	0.056	100
25	29	291	762	0.390	92.9	10	40	119	0.010	264.3	5	126	233	0.030	53.5
50	14	159	413	0.114	27.2	8	38	111	0.009	228.9	3	113	178	0.015	26.4
75	9	99	274	0.051	12.2	5	39	74	0.003	83.2	2	90	139	0.009	15.6
100	5	60	135	0.011	2.7	1	8	12	0	1.7	1	52	78	0.003	4.7
Cone 5, 1,250 μm															
0	44	589	1,463	1.409	100	6	39	107	0.008	100	7	273	431	0.087	100
25	24	229	722	0.368	26.1	9	36	119	0.010	129.6	6	192	347	0.066	75.1
50	10	76	262	0.049	3.5	2	9	22	0	4.1	3	100	180	0.018	20.1
75	8	68	208	0.030	2.2	0	0	0	0	0.0	2	74	127	0.008	9.6
100	4	45	111	0.008	0.6	0	0	0	0	0.0	1	30	54	0.002	1.8
Cone 6, 1,250 μm															
0	140	1,705	3,257	6.048	100	44	539	944	0.472	100	15	365	776	0.368	100
25	60	850	1,679	1.647	27.2	32	502	716	0.205	43.4	9	219	521	0.176	47.7
50	40	612	1,154	0.752	12.4	23	260	415	0.082	17.4	7	180	401	0.101	27.4
75	26	434	798	0.352	5.8	11	116	179	0.015	3.1	4	121	281	0.051	13.7
100	10	172	347	0.071	1.2	1	11	20	0	0.0	3	77	207	0.029	7.9
Cone 7, 1,500 μm															
0	156	1,818	3,738	8.378	100	35	300	568	0.183	100	13	305	583	0.194	100
25	106	1,306	2,779	4.726	56.4	49	528	909	0.430	235.4	13	239	682	0.320	165.3
50	65	859	1,805	1.979	23.6	28	347	535	0.130	71.3	11	275	578	0.203	104.7
75	55	660	1,566	1.584	18.9	16	135	253	0.036	19.7	6	173	395	0.099	51.1
100	25	352	701	0.289	3.4	10	93	167	0.015	8.3	5	148	309	0.058	29.8
Cone 8, 1,850 μm															
0	102	1,351	2,717	4.364	100	14	182	293	0.041	100	17	466	796	0.327	100
25	53	571	1,295	1.061	24.3	20	111	251	0.040	96.1	10	288	498	0.130	39.6
50	27	333	808	0.426	9.8	10	55	149	0.015	36.4	5	255	348	0.044	13.5
75	11	106	292	0.058	1.3	0	0	0	0	0.0	3	162	229	0.021	6.3
100	7	65	180	0.022	0.5	2	14	35	0.001	2.0	2	115	164	0.011	3.3
Cone 9, 2,050 μm															
0	150	1,923	3,622	7.399	100	57	425	780	0.336	100	27	571	1,203	0.881	100
25	67	737	1,524	1.398	18.9	30	200	379	0.081	24.2	12	301	714	0.329	37.4
50	30	311	731	0.344	4.6	16	113	221	0.028	8.4	8	202	480	0.149	16.9
75	20	187	482	0.155	2.1	8	48	120	0.010	2.8	5	128	366	0.092	10.5
100	6	72	165	0.017	0.2	0	0	0	0	0.0	1	45	89	0.005	0.5
Cone 10, 2,700 μm															
0	94	1,575	3,216	6.175	100	22	361	540	0.127	100	22	889	1,395	0.908	100
25	50	547	1,433	1.378	22.3	20	149	312	0.059	46.6	13	497	786	0.291	32.1
50	27	331	786	0.399	6.5	15	103	212	0.027	21.3	7	312	482	0.106	11.7
75	11	163	365	0.084	1.4	1	10	19	0	0.2	3	255	331	0.035	3.9
100	6	86	204	0.027	0.4	0	0	0	0	0.0	1	116	134	0.004	0.4
Cone 11, 3,350 μm															
0	139	1,700	3,289	6.226	100	26	252	397	0.074	100	26	496	988	0.573	100
25	93	873	2,127	2.955	47.5	52	332	670	0.266	359.9	15	391	699	0.264	46.0
50	33	331	820	0.442	7.1	18	110	223	0.030	40.0	9	303	473	0.104	18.1
75	20	228	587	0.230	3.7	10	57	127	0.010	13.7	5	222	343	0.054	9.4
100	6	71	187	0.024	0.4	2	20	35	0.001	0.9	2	127	168	0.009	1.7

Relative depth, depth down cone with base set at 0% and apex at 100%. *n*, No. of tubules measured; ID, sum of inner diameter of tubule (μm); OD, sum of outer diameter of tubule (μm); CSA, sum of cross-sectional cell surface area (mm^2). %CSA, percentage of total cross-sectional cell surface area.

Downloaded from ajpregu.physiology.org on July 31, 2007

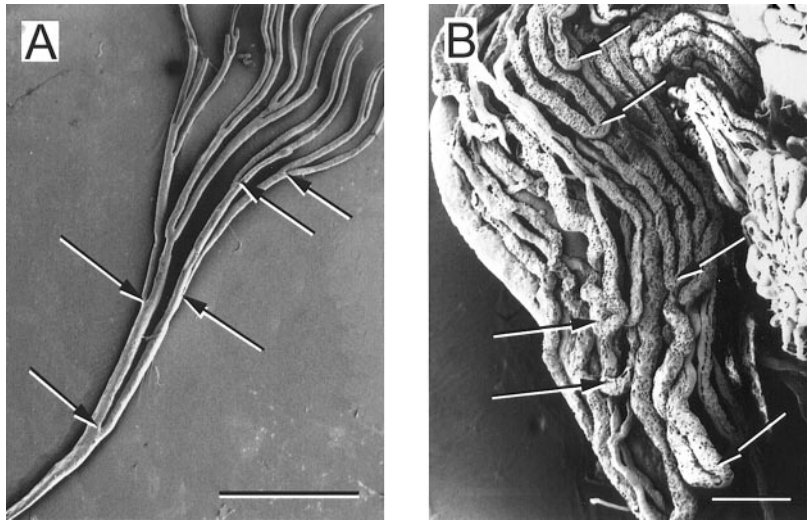

Fig. 2. *A*: scanning electron micrograph of a methyl methacrylate cast of the collecting ducts in a single medullary cone of a quail kidney. Arrows show points of convergence of collecting ducts. Note that the collecting ducts coalesce at distinct levels within the cone structure. *B*: scanning electron micrograph of a methyl methacrylate cast of the pattern of nephron loops within an avian medullary cone (Gambel's quail). Arrows show the turning points of looped nephrons. Note that the loops of Henle turn at differing depths within the medullary cone.

the tip of the medullary cones (Fig. 4*B*). At the midpoint of the cones ~75 ± 8.0% of the collecting ducts had disappeared. There was little correlation between the length of the cones and the number of collecting ducts at the base ($r = 0.18$, $P < 0.05$).

The structure of the descending limb of the loop of Henle was variable with respect to the length of the prebend thick and the thin descending segments of the loop among nephrons of the same length. The variation in the prebend thick segment was such that little correlation existed between the length of this segment and total loop length (Fig. 5*A*, $r = 0.27$). The length of the prebend segment from isolated nephrons ranged from 130 to 770 μm. However, the length of the thin limb of Henle was highly correlated with the length of the loop of Henle (Fig. 5*B*, $r = 0.99$). Among all isolated

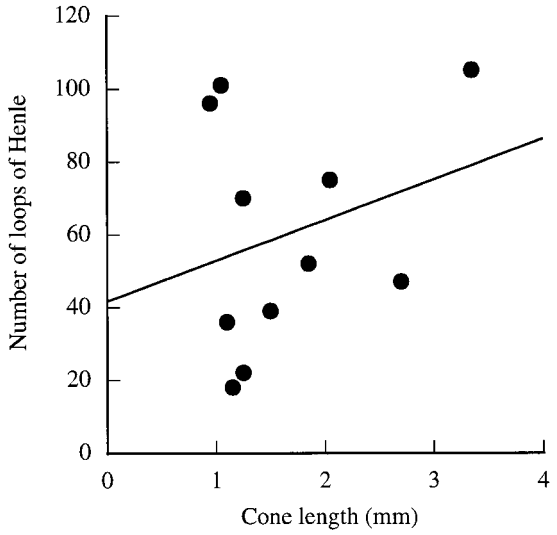

Fig. 3. The absolute number of nephrons at the base of the cone as a function of total cone length. The absolute number of nephrons was calculated by taking the number of descending and ascending limbs of Henle and dividing by two. The equation describing the regression line is $y = 32.1 + 16.2x$ ($r^2 = 0.137$).

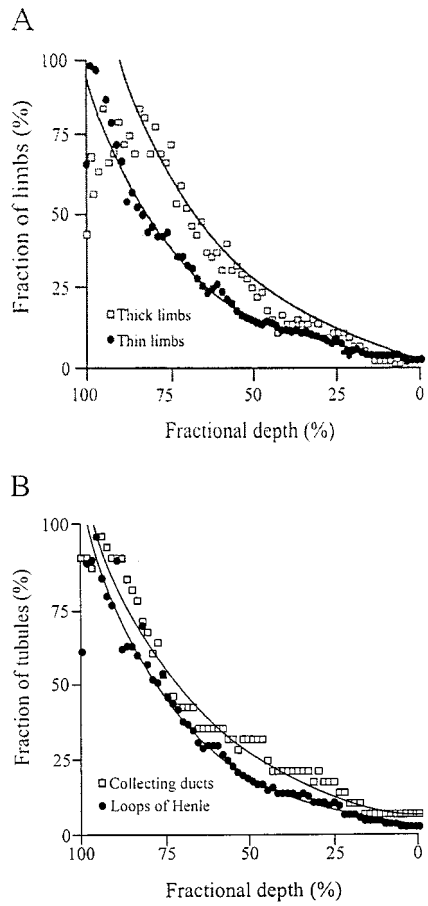

Fig. 4. *A*: fraction of thin descending limbs of Henle and thick ascending limbs of Henle as a function of fractional depth toward the apex of a representative medullary cone. *B*: fraction of collecting ducts and total number of nephrons (loops of Henle) as a function of fractional depth toward the apex of a representative medullary cone. In both *A* and *B*, cone 11 is represented. The number of tubule elements toward the apex of the cone is expressed as a fraction of those present at the corticomedullary boundary. The absolute length of the cone was set at 100%.

Downloaded from ajpregu.physiology.org on July 31, 2007

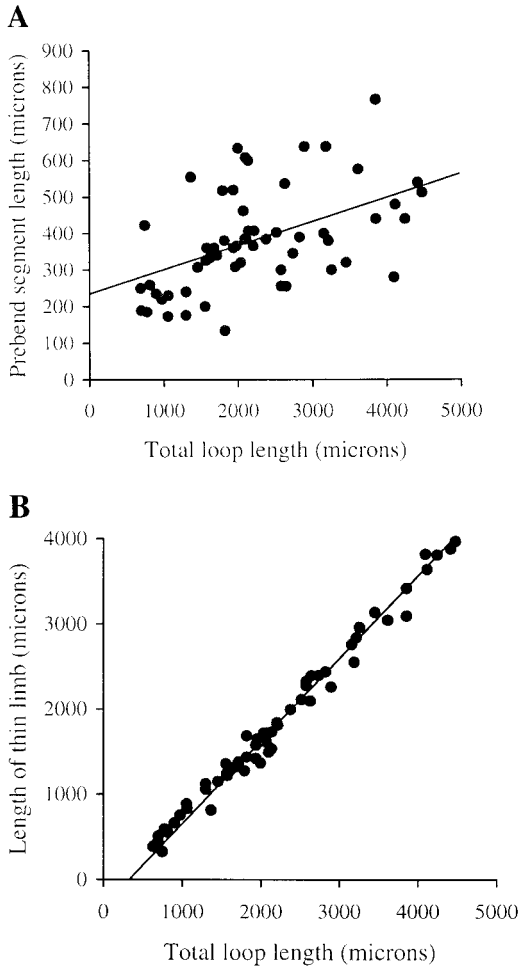

Fig. 5. *A*: length of the prebend thick segment as a function of loop of Henle length. The equation describing the line is $y = 223.9 + 0.07x$ ($r^2 = 0.27$). The length of the prebend thick segment and the total loop length do not appear to be interrelated. *B*: length of thin limb of Henle as a function of the total length of the loop of Henle (i.e., the length of the thin limb of Henle and the prebend segment). The equation describing the line is $y = 223.9 + 0.93x$ ($r^2 = 0.99$).

nephrons, the length of the thin limb ranged from 390 to 3,970 μm.

To obtain a measure of the ion transporting area of the epithelia at the levels of the cones analyzed the inner and outer diameters of the tubules were measured. These data were used to calculate the cross-sectional cell surface area of the individual tubules (descending and ascending limbs of Henle and collecting ducts). The formula for the surface area of an annulus was used to calculate the surface area of the tubules [$A = \Pi (r_1 + r_2) (r_1 - r_2)$, where $r_1 \geq r_2$]. At each level, the total cross-sectional cell surface area was calculated for each tubule type. The data are presented in absolute numbers and in relative terms with the measurements at the base of the cones taken as 100% (Table 1, Fig. 6).

The surface area occupied by each tubule element decreased toward the apices of the cones. However, for the thin limbs of Henles loop, the surface area present at 25% of the distance toward the apices the cones exceeded the area at the base of the cones by 17.5% (Table 1, Fig. 6). Beyond this point, surface area of thin and thick limbs of Henle and collecting ducts decreased in a similar manner as the apex of the cones was approached (Fig. 6).

Data on the number of tubules at each level were regressed against cone depth. The regression equations of the summarized data for all cones are presented in Table 2. These data were converted to log base 2. The exponent from each equation indicates the number of convergences of each collecting duct type as a function of fractional cone depth. For example, at the base of cone 11, there are 26 collecting ducts (Table 1). The exponent for collecting ducts for cone 11 indicates that on average there will be 4.11 convergences along the length of the cones (Table 2). Thus starting with 26 collecting ducts, after one convergence there will be 13, then 6.5, 3.25, and finally 1.6. This last value (1.6) is close to the actual value of two, which is the number of collecting ducts remaining near the apex of this cone (see Table 1).

Based on our observations and the data presented, a two-dimensional diagram is presented depicting the lengths of the loops of Henle as they may appear in the medullary cones (Fig. 7). The data indicate that most of the loops of Henle are rather short and that the lengths of the thin limb and prebend segment vary among nephrons. The length of the thin limb of Henle is greater in longer nephrons, and the length of the prebend segment is independent of the length of the loop of Henle.

DISCUSSION

In this study the general features of the renal medulla of the kidney of the desert quail were described and analyzed. The renal medulla of birds is divided into smaller units than occur for most mammalian kidneys. These units, medullary cones, are made up of loops of Henle, collecting ducts, and vasa recta. The individual cones function in much the same manner as the renal medulla of mammalian kidneys. The goal of

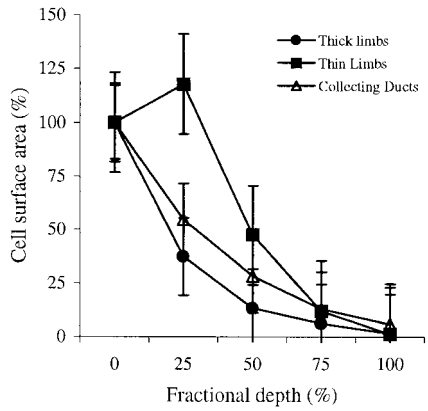

Fig. 6. Cross-sectional cell surface area vs. fractional depth toward the apices of the cones for thick and thin limbs of Henle and collecting ducts. The base of the cones was set at zero and the apex at 100%. Data are means ± SE for all cones.

Downloaded from ajpregu.physiology.org on July 31, 2007

Table 2. *Regression equations for the numbers of nephrons, thick limbs of Henle, thin limbs of Henle, and collecting ducts as a function of depth down the medullary cone*

Cone No.	Nephrons	Thin Limbs of Henle	Thick Limbs of Henle	Collecting Ducts
1	$1.01\times2^{-3.24x}$	$1.07\times2^{-3.54x}$	$0.99\times2^{-3.13x}$	$1.22\times2^{-3.37x}$
2	$1.13\times2^{-4.14x}$	$1.73\times2^{-5.97x}$	$0.99\times2^{-3.68x}$	$1.17\times2^{-3.19x}$
3	$1.26\times2^{-3.12x}$	$0.97\times2^{-2.55x}$	$1.19\times2^{-2.81x}$	$1.03\times2^{-3.02x}$
4	$1.06\times2^{-2.43x}$	$0.65\times2^{-1.14x}$	$1.07\times2^{-2.77x}$	$0.96\times2^{-3.09x}$
5	$1.15\times2^{-3.93x}$	$0.77\times2^{-2.57x}$	$0.98\times2^{-3.80x}$	$1.07\times2^{-3.70x}$
6	$0.99\times2^{-3.53x}$	$1.37\times2^{-4.04x}$	$0.88\times2^{-3.51x}$	$0.96\times2^{-2.49x}$
7	$1.29\times2^{-4.05x}$	$1.13\times2^{-3.56x}$	$1.07\times2^{-3.75x}$	$1.05\times2^{-3.70x}$
8	$1.38\times2^{-3.92x}$	$1.07\times2^{-3.42x}$	$0.93\times2^{-4.01x}$	$0.94\times2^{-3.34x}$
9	$1.00\times2^{-4.52x}$	$0.95\times2^{-4.42x}$	$0.92\times2^{-4.39x}$	$1.00\times2^{-4.00x}$
10	$1.25\times2^{-4.51x}$	$1.46\times2^{-5.28x}$	$1.03\times2^{-4.09x}$	$0.95\times2^{-3.88x}$
11	$1.09\times2^{-5.03x}$	$1.43\times2^{-4.91x}$	$0.95\times2^{-4.98x}$	$1.15\times2^{-4.11x}$

the present study was to more clearly determine the architecture of the medullary cones with the hope that the information would lead to a better understanding of the function of the countercurrent multiplier system within the avian kidney.

The cones analyzed in this study ranged in length from 950 to 3,350 μm. The data show that cone diameter is independent of cone length, which suggests that the number of loops of Henle entering a cone is also independent of cone length if it is assumed that a larger diameter would accommodate more loops. It follows that short cones may have a large number of loops and the converse is true for long cones.

One of the basic premises of the countercurrent multiplier theory as it applies to the kidney is that the longer the loops of Henle, the greater the multiplier effects. Therefore, the longer cones (with longer loops of Henle) should be able to conserve more water through the production of hyperosmotic urine. This has the potential of being beneficial, but the output from the longer cones is probably counterbalanced by the product of the shorter medullary cones, as the fluid from all cones eventually mixes in the ureteral branches and the ureter. This may be one factor that limits the maximum concentration of the urine produced by avian kidneys.

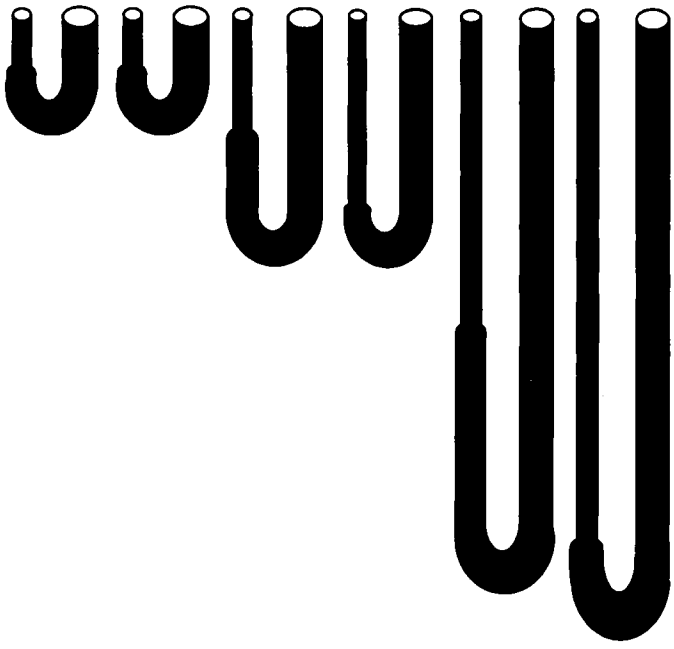

Fig. 7. Schematic representation showing pattern of the cascade of loop of Henle lengths that are present in the Gambel's quail medullary cone. Note that the majority of nephrons have a short loop of Henle and that the lengths of the thin descending limbs of Henle and prebend segments vary among the nephrons.

Studies on the countercurrent multiplier system of mammals suggest that a cascade in the lengths of the loops of Henle is important in the production of concentrated urine (15, 16). The cascade is produced by a decrease in the number of loops of Henle toward the apices of the renal medulla, which gives the medulla (or cone) a tapered shape. The fluid in the longer descending limbs equilibrates osmotically with the interstitium that has been rendered hyperosmotic by the action of the ascending limbs of shorter loops of Henle. Thus the shorter loops preconcentrate the fluid in the descending limbs of the longer loops of Henle as these limbs traverse the interstitium at the level of the shorter loops. The fluid in the descending limbs of the longer loops is further concentrated by equilibration with the interstitium of the deeper medulla. In modeling studies using data for the rat kidney, nephrons that turn too early or too late in the medulla lower the maximal concentrating ability of the cascade system (15, 16). In the rat the distribution of lengths in the loop of Henle population may be near optimal, allowing the system to work at peak efficiency as predicted by the cascade model (15). Similar simulations should be carried out with the data in the present paper to determine whether the loop population occurring in the quail kidneys allows for the most efficient function of this countercurrent multiplier system.

The single solute hypothesis for urine concentration in birds does not include a role for the prebend segment (19). However, more recently Layton and Davies (16) have hypothesized that the prebend segment may act in a manner similar to the diluting segment and aid in amplifying concentrating capacity. In Gambel's quail, the ultrastructure of this segment is similar to that of the ascending limb in that it is densely populated with mitochondria (21), suggesting that it may play a role in sodium chloride absorption. This in turn may aid in

Downloaded from ajpregu.physiology.org on July 31, 2007

developing an interstitial concentration gradient to enabling the passive reabsorption water from the collecting duct network thus producing hyperosmotic urine. Our findings indicate that this segment may be of a substantial length (up to 770 μm); hence the possible importance of this region of the nephron to the function of the countercurrent multiplier system should not be overlooked.

The observation that the number of loops of Henle in the medullary cones of the quail kidney decreases toward the tip of the medulla is consistent with those for the renal medulla of the rat and rabbit kidneys (13, 14). There is no region of the avian medullary cone that corresponds to the inner medulla that is present in most mammal kidneys (5). The data for the rat and rabbit kidneys show a decrease in number of thick ascending limbs of Henle and collecting ducts from the corticomedullary boundary to the boundary of the outer stripe of the outer medulla (13, 14). Thus it would appear that the avian medullary cones are structurally similar (analogous) to the outer medulla of mammal kidneys. The question remains as to whether these two areas function in a similar manner in avian and mammalian kidneys. Simulation based on the data presented here (and other data from the literature) may clarify this point.

In the medullary cones, the number of collecting ducts decreases as a function of length, but the inner and outer diameters of individual ducts increase with distance down the cones. The result is that toward the cone apices, there are fewer, larger collecting ducts. A similar pattern is found with the collecting ducts of rat and rabbit kidneys (14). Although the inner and outer diameters of individual collecting ducts increase with distance down the cones, the decrease in number of collecting ducts is such that the total cross-sectional area decreases with cone depth. The data for cross-sectional cell surface area of the thin and thick limbs of the loop of Henle follow the same pattern as that for the collecting ducts. The decrease in cross-sectional cell surface area seen for the limbs of Henle is in concert with the functional cascade that is apparently necessary for the efficient function of a renal countercurrent multiplier system. The increase in size (luminal diameter) of individual collecting ducts with distance down the cones may be related to the excretion of uric acid by the avian kidney. Uric acid is excreted as spheres that grow larger with transit through the renal tubules. They can reach a size of 15 μm as the late collecting ducts are reached (8).

Based on our data we present a qualitative representation of the morphology for the thin and thick limbs of Henle within the quail medullary cone (Fig. 7). This representation fulfils some of the parameters of our data: *1*) the numbers of thin and thick limbs of Henle decrease with distance down the cone, *2*) the most rapid decrease in the number of limbs occurs in the early part of the cone (near the base), *3*) the rate of decrease of thin limbs of Henle is greater than for the thick limbs, and *4*) the length of the prebend (thick) segment varies among adjacent nephrons.

In summary, the avian medullary cone presents a structural organization that is similar to the outer medulla of the mammalian kidney. Studies on the avian kidney that lacks the inner medulla may aid in determining the function of this region in the mammalian kidney.

Perspectives

Birds and mammals are the only vertebrates that can conserve body water by excreting solutes in greater concentrations than they occur in plasma, i.e., they produce urine hyperosmotic to plasma from which it was filtered. The hyperosmotic urine is formed in the medullary regions of these kidneys and is dependent on the process of countercurrent multiplication. To function, countercurrent multiplier systems require a system of parallel tubules arranged in close proximity. This arrangement has been studied for mammalian kidneys; however, similar detailed information for the avian kidney is lacking in the literature. In the study reported in this paper, the morphology of the quail medullary cone was examined as an example of the avian renal medulla. The results showed that the avian renal medulla is cone shaped due to the decrease in the number of loops of Henle that occurs as the apex of the medullary cones is reached. This result fits well with previous suggestions that the function of the avian countercurrent multiplier system would reach its peak efficiency with a cascade in the lengths of the loop of Henle. Therefore, the morphological data presented in this paper appears to substantiate earlier efforts to model the avian countercurrent multiplier system. Moreover, the data presented in this paper should serve as a foundation for future efforts to develop computer simulations that may in turn aid in suggesting future biological experiments. Such modeling work and experiments on the avian medullary cone have the potential to lead to a better understanding of the function of the mammalian renal medulla. This may be possible due to the relatively simpler medullary region and countercurrent multiplier in birds compared with mammals. This is derived from the observation that the avian countercurrent multiplier system has only one solute (sodium chloride) making up its osmotic gradient (most mammal system have two solutes, sodium chloride and urea) and the absence of a thin ascending segment of loop of Henle of the avian nephron.

This study was funded by the National Science Foundation Grant IBN-9220241.

REFERENCES

1. **Barrett JM, Kaissling B, and de Rouffignac C.** The ultrastructure of the nephron of the desert rodent (Psammomys obesus) kidney. II: Thin limbs of Henle of long-looped nephrons. *Am J Anat* 151: 499–514, 1978.
2. **Barrett JM and Majack RA.** The ultrastructural organization of long and short nephrons in the kidney of the rodent Octodon degus. *Anat Rec* 187: 530–531, 1971.
3. **Boykin SLB and Braun EJ.** Entry of nephrons into the collecting duct network of the avian kidney: a comparison of chickens and desert quail. *J Morphol* 216: 259–269, 1993.

Downloaded from ajpregu.physiology.org on July 31, 2007

4. **Braun EJ.** Renal response of the starling to an intravenous salt load. *Am J Physiol Renal Fluid Electrolyte Physiol* 234: F270–F278, 1978.
5. **Braun EJ and Dantzler WH.** Function of mammalian-type and reptilian-type nephrons in kidneys of desert quail. *Am J Physiol* 222: 617–629, 1972.
6. **Braun EJ and Dantzler WH.** Effects of ADH on single-nephron glomerular filtration rates in the avian kidney. *Am J Physiol* 226: 1–8, 1974.
7. **Braun EJ and Dantzler WH.** Effects of water loading on renal glomerular and tubular function in desert quail. *Am J Physiol* 229: 222–227, 1975.
8. **Casotti G and Braun EJ.** Ionic composition of urate-containing spheres in the urine of domestic fowl. *Comp Biochem Physiol A* 118: 585–588, 1997.
9. **Chou C-L, Nielsen S, and Knepper MA.** Structural-functional correlation in chincilla long loop of Henle thin limbs: a novel papillary subsegment. *Am J Physiol Renal Fluid Electrolyte Physiol* 265: F863–F874, 1993.
10. **Dantzler WH and Braun EJ.** Comparative nephron function in reptiles, birds, and mammals. *Am J Physiol Regulatory Integrative Comp Physiol* 239: R197–R213, 1980.
11. **Emery N, Poulson TL, and Kinter WB.** Production of concentrated urine by avian kidneys. *Am J Physiol* 223: 180–187, 1972.
12. **Goldstein DL and Braun EJ.** Structure and concentrating ability in the avian kidney. *Am J Physiol Regulatory Integrative Comp Physiol* 256: R501–R509, 1989.
13. **Han JS, Thompson KA, Chou C-L, and Knepper MA.** Experimental tests of three-dimensional model of urinary concentrating mechanism. *J Am Soc Nephrol* 2: 1677–1688, 1992.
14. **Knepper MA, Danielson RA, Saidel GM, and Post RS.** Quantitative analysis of renal medullary anatomy in rats and rabbits. *Kidney Int* 12: 313–323, 1977.
15. **Layton HE.** Distribution of Henle's loops may enhance urine concentrating ability. *Biophys J* 49: 1033–1040, 1986.
16. **Layton HE and Davies JM.** Distributed solute and water reabsorption in a central core model of the renal medulla. *Math Biosci* 116: 169–196, 1993.
17. **MacMillen RE and Lee AK.** Australian desert mice: independence of exogenous water. *Science* 158: 383–385, 1967.
18. **MacMillen RE and Lee AK.** Water metabolism of Australian hopping mice. *Comp Biochem Physiol* 28: 493–514, 1969.
19. **Nishimura H, Koseki C, Imai M, and Braun EJ.** Sodium chloride and water transport in the thin descending limb of Henle of the quail. *Am J Physiol Renal Fluid Electrolyte Physiol* 257: F994–F1002, 1989.
20. **Poulson TL.** Countercurrent multipliers in avian kidneys. *Science* 148: 389–391. 1965.
21. **Reimer PR and Braun EJ.** Structure of avian loop of Henle as related to countercurrent multiplier system. *Am J Physiol Renal Fluid Electrolyte Physiol* 255: F500–F512, 1988.
22. **Roy DR, Layton HE, and Jamison RL.** Countercurrent mechanism and its regulation. In: *The Kidney: Physiology and Pathophysiology* (2nd Ed.), edited by Seldin DW and Giebisch G. New York: Raven, 1992, p. 1649–1692.
23. **Sands JM and Layton HE.** Urine concentrating mechanism and its regulation. In: *The Kidney: Physiology and Pathophysiology* (3rd Ed.), edited by Seldin DW and Giebisch G. Philadelphia: Lippincott Williams & Wilkins, 2000, p. 1175–1216.
24. **Sasaki Y, Takahashi T, and Suwa N.** Quantitative structural analysis of the inner medulla of rabbit kidney. *Tohoku J Exp Med* 98: 21–32, 1969.
25. **Skadhauge E and Schmidt-Nielsen B.** Renal medullary electrolyte and urea gradient in chickens and turkeys. *Am J Physiol* 212: 1313–1318, 1967.
26. **Stephenson JL.** Urinary concentration and dilution: models. *Handbook of Physiology. Renal Physiology*. Bethesda, MD: Am Physiol Soc, 1992, vol. 2, p. 1349–1408.
27. **Stephenson JL, Zhang Y, and Tewarson R.** Electrolyte, urea, and water transport in a two-nephron central core model of the renal medulla. *Am J Physiol Renal Fluid Electrolyte Physiol* 257: F338–F413, 1989.
28. **Wexler AS, Kalaba RE, and Marsh DJ.** Three-dimensional anatomy and renal concentrating mechanism. I. Modeling results. *Am J Physiol Renal Fluid Electrolyte Physiol* 260: F368–F383, 1991.
29. **Williams JB, Pacelli MM, and Braun EJ.** The effect of water deprivation on renal function in conscious unrestrained Gambel's quail (Callipepla gambelii). *Physiol Zool* 64: 1200–1216, 1991.

Downloaded from ajpregu.physiology.org on July 31, 2007